Multi-Threshold Hausdorff Distance with Maximal Arc-Length Matching for Variational Shape Recognition

Anjan Goswami and Amitabha Mukerjee
Department of Mechanical Engineering,
IIT Kanpur
{anjan,amit}@iitk.ac.in

Abstract

Widely varying shapes are difficult to recognized especially when present as part of an occluded shape. Handling such situations requires the consolidation of data at different levels of confidence, which is encoded in a novel Hausdorff Distance-based measure of planar shape similarity. Given two sets of features M and I, the directed Hausdorff measure from M to I is the maximum among the closest match for each feature of M, With variations in the features, this approach tends to emphasize the outliers, which has led to suggestions of taking the k-th minimum measure as a matching function [5, 12]. The parameter k can be avoided by computing the fraction of the model present at a given threshold, which has been called the Hausdorff Fraction [11]. However, this depends on the choice of the threshold parameter.

In this work, we develop a novel method for avoiding this threshold by using multiple thresholds (MUT) and combining the data from different levels of confidence. The choice of the differing thresholds is also shown not to affect the model. Further improvement on the model is obtained using the Maximal Arc-Length (MAL) criterion, where subsequent segments, if matching, lend greater validity to the match.

The combined algorithm (MUTMAL) has been implemented on the polygonal domain, in which variational shape classes have been generated using vertex and edge deformation from a nominal model. The polygon contour is modeled with supersegments (chains of edges represented by relative length and angle). Where the variations are large, or the contour may be occluded to a high degree, the search model using a combination of maximal arc-length matching and the Multi-Threshold Hausdorff fraction appears to be very robust.

KEYWORDS: Shape, Object Recognition, Hausdorff Distance

Multi-Threshold Hausdorff Distance with Maximal Arc-Length Matching for Variational Shape Recognition

Abstract

Widely varying shapes are difficult to recognized especially when present as part of an occluded shape. Handling such situations requires the consolidation of data at different levels of confidence, which is encoded in a novel Hausdorff Distance-based measure of planar shape similarity. Given two sets of features M and I, the directed Hausdorff measure from M to I is the maximum among the closest match for each feature of M, With variations in the features, this approach tends to emphasize the outliers, which has led to suggestions of taking the k-th minimum measure as a matching function [5, 12]. The parameter k can be avoided by computing the fraction of the model present at a given threshold, which has been called the Hausdorff Fraction [11]. However, this depends on the choice of the threshold parameter.

In this work, we develop a novel method for avoiding this threshold by using multiple thresholds (MUT) and combining the data from different levels of confidence. The choice of the differing thresholds is also shown not to affect the model. Further improvement on the model is obtained using the Maximal Arc-Length (MAL) criterion, where subsequent segments, if matching, lend greater validity to the match.

The combined algorithm (MUTMAL) has been implemented on the polygonal domain, in which variational shape classes have been generated using vertex and edge deformation from a nominal model. The polygon contour is modeled with supersegments (chains of edges represented by relative length and angle). Where the variations are large, or the contour may be occluded to a high degree, the search model using a combination of maximal arc-length matching and the Multi-Threshold Hausdorff fraction appears to be very robust.

1 Introduction

This paper considers model based planar shape recognition in a cluttered and occluded environment where the sample of models present in the input shape may be occluded or deformed. Hausdorff distance based approaches have been widely used for computing distance measure between two feature sets. The hausdorff distance model is powerful enough to capture partial instances of models, but it has a potential drawback when recognizing variational shape classes under occlusion. In case of variation and occlusion the features of models in the input shape may get corrupted and it becomes difficult to estimate the parameters of Hausdorff distance. We present a de-parametrized multi-threshold model of hausdorff fraction where the decision is based on cumulative error in multiple error zones instead of any threshold parameters. We also show that choice of differing error zones do not affect the efficacy of the algorithm. Further, we consolidate this multi-threshold directed hausdorff distance approach with maximal arc-length matching which is shown to be very robust against variation. In practice, since length is scale dependent, we maximise the number of segments matched.

One of the pre-requisites in testing variational shape matches is the generation of variational shape classes for testing. Here we use variations on the contours of 2D polygons based on edge and vertex perturbation as a simple but effective model for shape variation (Section 3 compares this and other variational shape class models). Test results from this domain demonstrate successful recognition in some of the worst input shapes.

2 Hausdorff Distance

The directed Hausdorff measure from M to I, where M and I are point sets,is $h(M, I) = \max_{m \in M} \min_{i \in I} \parallel m - i \parallel$. This can be better visualized as a set containment problem where $h(M, I) \leq \delta$ implies that M is contained within a set obtained by offsetting I by a open disk of radius δ.

In the context of model based shape recognition, this is used to compute distance between feature sets of a model shape to an input shape. This measure gives the maximum distance of a feature in set M from its closest feature in set I. For example, if M and I are polygons represented by relations between successive segment sequences then distance between two features is a suitable norm of the difference in these relations.

2.1 Polygon Shape Distance

Success of any recognition scheme also depends on data representation. For polygons, the supersegment representation [14] provides a translation, rotation and scaling invariant representation and saves us from complex searches for optimally superimposing the models on the input shape. Supersegments are successive sequences of edges of the polygons. The number of composing segments ν is the cardinality of the supersegment. The relative length ratios and included angles with each of the ν preceding edges results in a 2ν-tuple feature vector for a given edge.

For supersegment features, while comparing the i-th feature of the model M and image I, a weighted error norm may be defined as follows:

$$\frac{1}{2\nu}\left[\sum_{j=i,p=q}^{i-k,q-k}\left(w_l|L_j^I - L_p^M|^n + w_\theta|\theta_j^I - \theta_p^M|^n\right)\right]^{1/n}$$

, where $L_j^I = l_j/l_{j-1}$; ^{I} and ^{M} denote the input and model shapes. Initial experiments fail to find significant differences by weighting or by exponentiation, so the following results are reported only for with $w_l = w_\theta = 1$ and the exponent $n = 1$ also, which reduces it to the norm of order 1.

M-0	M-1	M-2	M-3	M-4
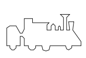				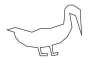
62	30	26	15	32
M-5	M-6	M-7	M-8	M-9
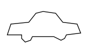	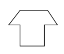		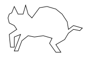	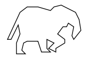
18	8	17	40	37
M-10	M-11	M-12	M-13	M-14
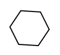	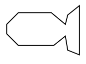	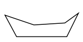		
6	12	6	56	18

M-15	M-16	M-17	M-18	M-19
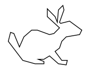	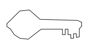			
37	27	41	43	8
M-20	M-21	M-22	M-23	M-24
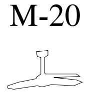	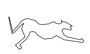	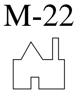		
24	51	15	10	15
M-25	M-26	M-27	M-28	M-29
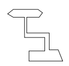	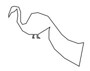			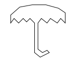
18	39	24	13	26

Table 1: Database of Model Shapes (number of edges below each figure).

2.2 Hausdorff Distance Variants

In general, the Hausdorff distance model is highly sensitive to even a single outlier in the portion of model shape present in the input shape. A partial Hausdorff measure [5] is thus often used. It is given by

$$h_k(M, I) = k{-}th \min_{m \in M} \min_{i \in I} \parallel m - i \parallel$$

when k−th min is the k−th minimum. k = n would result in the maximum value or the traditional hausdorff model.

This determines the Hausdorff measure among the k model features that are closest to input shape features. k can be set to a minimum number of model features (k-th) but this number should vary with the number of model features; an alternative model as a fraction of model features (% k) is not robust for models with very few features. In the latter case we may end up comparing the 15-th minimum match of a 30-sided model with the 3rd minimum match for a 6 sided model. On the other hand, the constant k model may have only 6 edges in which case models with many features have a higher probability of finding an accidental match. If this particular variant is to be adopted, we feel that a better measure can be to use the sum of first k minimum measures (Σ_k). This provides a better discrimination since it includes the results from the best matches also; these are typically lower for a correct match, whereas the k-th minimum may be noisy and high.

2.3 Multi-Threshold Hausdorff Fraction model (MUT)

Another variant of Hausdorff distance can be defined as the maximum number of features in the model such that the distance is below a given error threshold,

$$h_k(I, M_j) \leq \psi$$

. Let $k_\psi(I, M)$ denote the maximum k for which the above relation is true, and $\| M \|$ is the number of features in M. The ratio

$$F_\psi(I, M_j) = \frac{k_\psi\,(I, M_j)}{\| M_j \|}$$

reflects the fraction of the shape M present in I at the confidence indicated by the threshold ψ [11]. Though, this model avoids the problem of choosing a minimum k, it introduces another parameter ψ. Some prior knowledge of the likelihood of various model positions can be used to increase the efficiency of the search, but estimation of ψ remains a difficult problem for variational shape recognition, especially where we do not have any prior knowledge about the extent of variation of occlusion.

Our initial experiments with the different variants of Hausdorff Distance outlined above (see Tables 3, 5) led us to conclude that it is unlikely that any model with a single confidence level (single threshold cutoff) would be able to identify data in variational models, where different features may agree to differing degrees. We feel that it is necessary in such cases to fuse the conclusions that can be arrived by consolidating the data from different levels of confidence, and the proposed multi-threshold (MUT) directed Hausdorff Distance model attempts this very objective.

The multi-threshold fraction $F(M_j, I)$ sums the fractions at differing levels of error $\psi_0, \psi_1, \ldots, \psi_\mu$:

$$F_{MUT}(M_j, I) = 1/\mu \left(\sum_{i=0}^{i=\mu} F_{\psi_i}(M_j, I) \right)$$

Since the matches at low values of ψ are also present in the higher values, these edges get reinforced more than features detected for higher ψ which may contain some noise.

2.4 Maximal Arc-Length matching (MUTMAL)

Traditional feature-based approaches to recognition consider the matches of the shape features separately, and make no attempt to consolidate these. When the shape is decomposed into independent features, the relative positions of these features is lost. In reality however, the overall layout of features, which may be called the "gestalt", remains an important if not crucial element in performing the overall shape matching.

The Multi-Threshold model outlined above also similarly returns a set of features which match at differing levels of confidence, but no correlation is sought between the relative positions of these features. A little deliberation reveals that it is a simple matter to increase the measure of the match if the features being detected happen to constitute successive segments in a polygon boundary. More generally, if the j-th and (j+t)-th Input shape features are found to be closest to the i-th and (i+$t\prime$)$-$th Model features present within a specific error threshold, then $t = t\prime$ represent a corresponding match in the two contour chains. This is considered to be a arc-length maximizing match, and if p_{ψ_i} such matching pairs occur among k candidates of model features which are found within the threshold ψ_i, then the amount $2p_{\psi_i}/||M||$ is added to the Multi-Threshold (MUT) Hausdorff fraction to obtain the *Maximal Arc-Length enhanced Multi-Threshold* (MUTMAL) measure. The overall value of the combined MUTMAL measure then is

$$MUTMAL(M_j, I) = \frac{1}{\mu}(\sum_{i=0}^{i=\mu}(F_{\psi i}(M_j, I) + 2p_{\psi_i}/||M||))$$

Note that p_psi is the number of matching pairs and not the number of matching edges; thus if r edges from the Model match successively with r edges from the Image (with a constant shift of t), then $\binom{p_psi=r}{2}$, which can quickly overwhelm the simple sum of feature contribution of MUT resulting from no sequential matches.

In addition, as in the Multi-Threshold Fraction model, the more robust matches are also present in the higher thresholded, and thus contribute to p_psi over and over again.

2.5 Model Parameters

2.5.1 Error Threshold Values

The premise of the multi-threshold model - that of removing the choice of parameters - would be obviated if the values of the discretization μ or the values of the actual error thresholds ψ_j were to become critical. The model was formulated on the belief that cumulative data over multiple thresholds would remain more or less the same if the intervals changed. Repeated experiments have demonstrated the correctness of this premise and a sample with different error interval schemes is shown in Table 1 Furthermore, as the error threshold increases, more and more

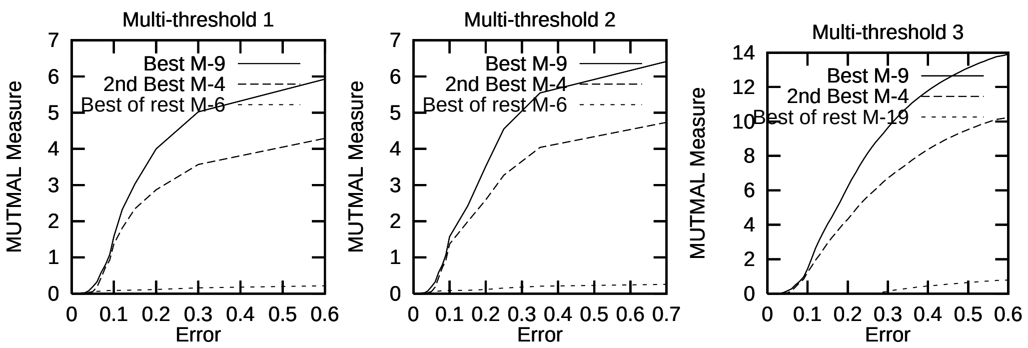

Figure 1: *Results of varying error zone. The left two represent 15 error thresholds in two different increasing intervals; the right has 60 uniform intervals, resulting in a smoother curve that is nonetheless quite similar.*

noisy data will enter and the rate of growth flattens out. This implies that the maximum error threshold ψ_μ is also not very critical. In the experiments that follow, we have used $\mu = 15$ and error thresholds with a maximum threshold $\psi_\mu = 0.6$, in a geometric thresholding scheme (higher errors correspond to a longer error interval). However, as noted in Table 1 the results are more or less identical for differing choices of these numbers.

2.5.2 Polygon Supersegment Length

The supersegment length ν used is a parameter for the particular choice of data representation, and is not a parameter in the Hausdorff Distance formulation as such. It reflects the number of consecutive elements represented in a single feature vector; thus each attribute is a local relation with ν preceding edges. Let l_i be the length of the i-th edge of a simple n-sided polygon. Then the feature attribute for ith edge is the 2ν-tuple shown here for ν = 2: $\{l_i/l_{i-1},\ l_i/l_{i-2},\ \theta_{i,(i-1)},\ \theta_{i,(i-2)}\}$, where $\theta_{i,j}$ is the included angle between edge-i and edge-j.

Within the supersegment model for polygon matching, the choice of such a parameter is inescapable. The larger the supersegment length ν, the more information would be corrupted near the intersections of occluded shapes, but the match will be more robust elsewhere. For models with high variation, a higher supersegment length consolidates information from a broader region of the contour and acts (a kind of low-pass filter), and is more robust (see Table 6. Where not indicated otherwise, ν=3 has been used in the following.

3 Shape Classes

Shape is defined in the dictionary as "constant relations of positions and proportionate distance among all the points composing its outline or its external surface,”[OED]. In this sense, shape may be defined as an equivalence class, where two shapes are equivalent if and only if there exists a constant relation $f()$ mapping all corresponding sets of points (“proportionate”) under transformations $C()$ such as rotation, translation and scaling:

$$S = S' \text{ iff } \forall (x, y) \in S \ \{\exists\ (x', y') \in S' \text{ s.t. } x' = C(x), y' = C(y) \text{ and } f(x, y) = f(x', y')\}$$

This definition identifies shape as a global property. In many applications in pattern recognition however, shape is not considered a constant: “leaving figures unaltered in ’unimportant’ ways” [6]. Whether a variation is important or unimportant is application specific Shock Graphs [4, 7], Parametric Boundary variation [2, 10], Manufacturing Tolerance models [13], Axis models [1].

E-varied	Shapes	V-varied	Shapes
E0101	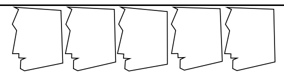	V05	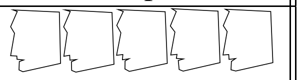
E0501	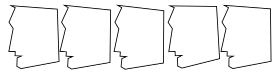	V10	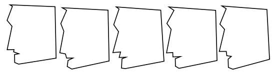
E0505	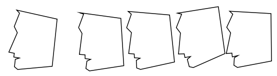	V20	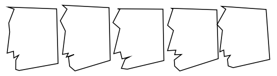
E0510	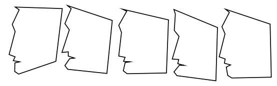	V30	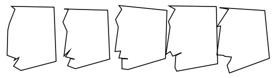
E1515		V45	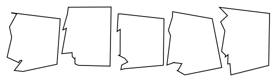

Table 2: Variational Class of face E: 0101 : Edge variation with length tolerance 1% of the average edge length and angle tolerance 1% of $\pi/18$. V: 05: Vertex type variation with a tolerance of 5% of average edge length of the polygon.

3.1 Variational Shape Class

For our domain of 2D polygonal shapes represented by their boundary, shape classes are generated by two simple deformations on the contour. Two types of deformation have been incorporated:

- *Vertex deformation* perturbs each vertex within a rectangular tolerance zone of same aspect ratio as the nominal shape. This is expressed as a percentage of the bounding box.

- *Edge or Chain variation* is varying the normalized (by perimeter) edge lengths and the turning angles from preceding edge within a specified tolerance zone. Here input shape is represented as a closed chain of edges;

each chain element being a relation with one or more preceding edges (the supersegment). When the chain is represented with discretized angles (e.g. 0,45°), then this results in the well known chain-code. The degree of variation in the edge is represented by the percentage of a standard angle (here $\pi/18$) and the edge-length variation expressed as a percentage of the average edge-length.

To ensure that all Images generated by this procedure are consistent, any self-intersecting or open polygonal chains arising from this procedure are pruned from the image set.

3.2 Overlapping Shape Classes

Shape class problems may be considered in many flavours:

- *Isolated Shape Contours.* The complete closed contour is available for matching, but may vary within the shape class.
- *Partial Shape Contours.* Here a part of the shape contour is available as an open chain.
- *Overlapping Shape Contours.* Here only a subset of the model contour is present in the image, but it is not known which part it is.

All three cases have been tested with all the variants of the Hausdorff Distance Paradigm discussed above. The greatest challenge however arises in the problem of occlusion where the test image may be constituted from a number of models, each of them having been deformed to differing degrees. Even in the simple domain of polygon recognition, this is recognized as a difficult problem. Whereas considerable work has been done on occluded shapes [3, 8], and on shape class recognition [9, 7], the problem of recognizing a variational shape when it is occluded has not been formally modeled, either from the shape class perspective or from the recognition perspective.

In considering overlapping shape classes, one must construct a measure for the degree of overlap of two shapes. One may measure area occlusion (area$(A \cap B) \div$ area $(A \cup B)$) or perimetric occlusion = (peri$(A \cap B) \div$ peri $(A \cup B)$). While this measure is easily generalized for three or more shapes, it does not reflect the asymmetric occlusion of different shapes - e.g. a small shape may be lost to the extent of 90% by area whereas the occlusion may be shown as 10%. An alternate measure may be to reflect the individual occlusions of each shape, but this involves $\binom{n}{2}$ relations for n objects. The results reported here use perimetric occlusion since the models are contour based.

4 Hausdorff Distance Models: Comparative Evaluation

This section reports the results of applying different directed Hausdorff model formalisms to the problem of variational shape recognition. A similar feature matching algorithm is adopted in all cases, the objective of which is to obtain an overall measure for the degree of match between a given input Image I and each of the models M_j in the model database. The main steps in the process are outlined for the MUTMAL measure, but

E-1							E-8						
M	Σ_k	k-th	%k	M	F_{MUT}	+MAL	M	Σ_k	k-th	%k	M	F_{MUT}	+MAL
0	.00	.00	.00	0	0.57	17	15	.01	.00	.00	15	0.71	17.03
28	.00	.00	.00	28	0.77	4.50	9	.25	.06	.08	9	.34	4.94
25	.70	.14	.14	25	0.17	0.23	4	.34	.07	.09	4	0.29	1.45
1	.93	.22	.27	27	0.10	0.164	0	.77	.16	.25	14	0.14	0.24
26	1.03	.23	.32	16	0.11	0.158	8	.85	.17	.25	8	0.12	0.19
15	1.05	.25	.32	6	0.15	0.150	26	.97	.18	.23	26	0.12	0.17
3	1.07	.27	.26	5	.11	2.11	18	.98	.20	.25	3	0.15	0.16

Table 3: *Results for some easy-to-recognize cases.* Both constituents in E-1 and the M-15 in E-8 are exact and results in zero error for several H.D. variant measures. M: Best matching models sorted by Σ_k and Multi-Threshold Maximal Arc-Length (+MAL).

the other models are also very similar:

- Construct a list of closest input feature with each feature in each model and store the edge number of the input shape matching with each of the model edge in a model shape.
- Construct error thresholds ψ_j and store the model features which are below the error threshold. Add votes for Maximal-Arc-length matching in each error-interval.
- The cumulative value of the MUTMAL measure for each error threshold is the sum of the measure for all previous bins plus the current bin.

4.0.1 Model Database

We use a database of 30 hand-drawn model shapes (Table 1). Table 2 shows some samples of generated variational shape classes and table 4 shows 8 experimental shapes. The constituent shapes of E1 and E2 exact. E-3, E-4, E-5, E-6 and E-8 consist of samples of shape classes. E-7 has some meaningless segments and

E-1	E-2	E-3	E-4	E-5	E-6
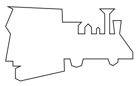	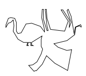		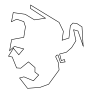	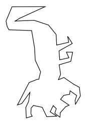	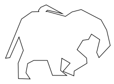
50 edges	80 edges	58 edges	55 edges	63 edges	47 edges
P.O: .52	P.O: .10	P.O: .25	P.O: .33	P.O: .14	P.O: .63
exact	exact	V:05 both	V:05 both	V15,V20	V05 both
E-7	E-8	E-9	E-10	E-11	E-12
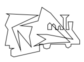		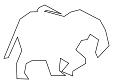	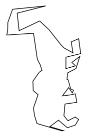	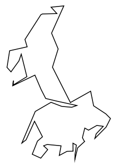	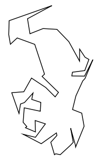
80 edges	58 edges	45 edges	54 edges	63 edges	62 edges
M-0, M-28	M-4, M-9	P.O: .67	P.O: .36	P.O: .16	P.O: .18
noise	and M-15	V:05 both	V:25 both	V:40 both	V50 both

Table 4: Experimental Images (I): Below each Image; Total Number of Edges, Perimetric Occlusion, models present, and shape variation. E-1, E-2, E-3 are exact shapes, whereas both E-4 and E-5 are from shape classes with 5% vertex variation. In E-6, the elephant has 20% and duck has 15% vertex variation. E-7 has some extra segments (which are present in none of the models). E-8 has three shapes - the elephant and duck have 5% vertex variation and the rabbit shape is exact.

E-2				E-3				E-4				E-7		
Σ_k	k.th	F_{MUT}	+MAL	Σ_k	k.th	F	+MAL	Σ_k	k.th	F_{MUT}	+MAL	Σ_k	k.th	F_{MU}
.00	.00	.82	16.94	.24	.05	.35	5.92	.22	.05	.42	9.30	.00	.00	.57
.00	.00	.81	13.10	.26	.06	.37	4.29	.30	.07	.27	1.57	.00	.00	.71
.12	.03	.16	0.16	.73	.16	.21	0.22	.78	.16	.20	0.20	.80	.19	.17

Table 5: *Results for some more simple cases*: E-2 (with M-17, M-26, M-8), E-3 (with M-9,M-4, M-0),E-4 (M-9, M-4, M-0), E-7(with M-0, M-28, M-25). For each case first two models are constituent candidates; the "best of the rest" model is also reported for comparison.

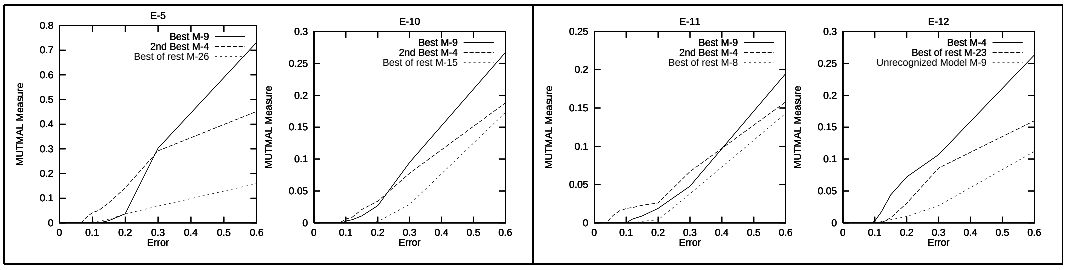

Figure 2: *Effect of high variation.* As the variation from the model shapes increases, the "best of the rest" (a model not actually present in the shape) approaches that of a model present due to high noise levels. Observing figures E-11 and E-12 in Table 1 tells us why.

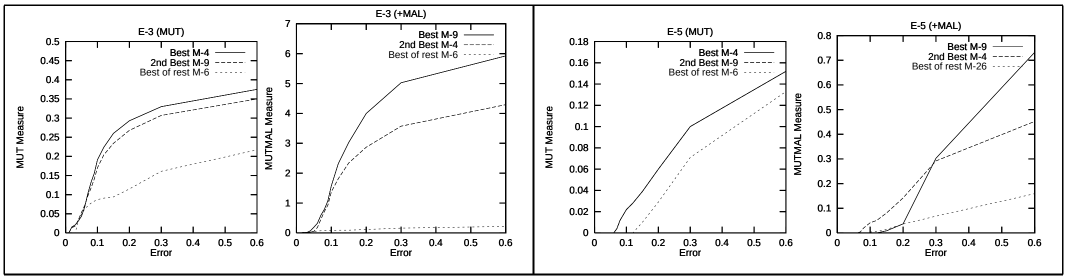

Figure 3: *Additional Effect of Maximal Arc-Length.* The results at different error zones for the Hausdorf Fraction with Multi-Threshold F_{MUT} (left), and for together with Maximal Arc-Length ("+MAL", right).

the E-8 has three shapes (two samples of shape classes and one exact). Table 3 reports results of sum of k, k minimal and fraction k model. Table 5 shows results of the recognition algorithm with E-2, E-3 and E-7.

4.1 k−th Hausdorff distance

We report the results for two mechanisms, used for choosing $k : k = 0.3\times$ number of edges (%k); or a fixed number less than the minimum number of edges in the model set (k-th). In the former case it may be different for different model shapes; thus we may end up comparing the 15-th minimum match of a 30 sided model with the 3rd minimum match for a 6 sided model. On the other hand, the simplest model may have only 5 edges in which case the larger models have a higher probability of finding an accidental match. It is also clear that the superseg-ment length ν must be less than k. In this work, in addition to the k-th minimum error, we found it more useful to consider another norm based on the sum of the k minimum measures (Σ_k). This provides a better discrimination if the best matches are small but the k-th minimum may be high.

The results for the various cases have been compared with the Multi-Threshold

$\nu = 2$			$\nu = 3$			$\nu = 4$		
M	Σ_k	k-th	M	Σ_k	k-th	M	Σ_k	k-th
4	.67	.17	4	.80	.22	9	1.45	.26
0	.78	.16	26	1.19	.24	4	1.49	.30
26	.81	.18	9	1.4	.25	26	1.59	.35
9	.86	.16	14	1.52	.31	26	1.59	.35
2	.89	.22	3	1.53	.292	29	1.88	.47

Table 6: *Results for E-5 with varying ν.* Even this mildly varying model cannot be recognized by the standard H.D. variants; only Σ_k model can recognize it with a longer supersegment length. The MATMUL results for this case ($\nu = 3$) are reported in the first column of Table 7.

E-5			E-10			E-11			E-12		
M	F_{MUT}	+MAL	M	F_{MUT}	+MAL	M	F_{MUT}	+MAL	M	F_{MUT}	+MAL
9	.13	.72	9	0.11	.27	9	.09	.20	4	.12	.26
4	.15	.45	4	0.12	0.19	4	.11	.16	23	.13	0.16
26	.11	.16	15	0.08	0.17	8	.08	0.14	8	0.09	0.15
8	.10	.15	26	0.10	.15	25	.10	.14	1	0.11	0.14
27	.12	.14	0	0.09	0.14	10	.13	.13	10	.13	.13

Table 7: *Comparative Evaluation of H.D. variants under Increasing Variation.* The data for +MAL tallies with the 0.6 error level in Figure **??**. Even in E-11, where the duck shape is hardly recognizable even by humans, the algorithm manages to find it (barely!). It fails however, in E-12, where the elephant model (M-9) does not even appear in the top 5.

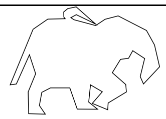 E-9							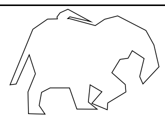 E-6						
M	Σ_k	k-th	%k	M	F_{MUT}	+MAL	M	Σ_k	k-th	%k	M	F_{MUT}	+MAL
9	.25	.05	.07	9	0.42	9.17	9	.25	.05	.07	9	0.41	9.61
4	.35	.09	.24	4	0.19	0.43	4	.56	.23	.29	4	0.15	0.26
29	.87	.18	.21	14	0.11	0.23	29	0.87	0.18	0.21	14	0.11	0.19
0	.89	.20	.30	3	0.13	0.20	13	.96	.21	.27	18	0.09	0.19
26	.96	.19	.29	18	0.10	0.19	26	1.0	.20	.32	6	0.18	0.18

Table 8: *Comparative Evaluation of H.D. variants under Increasing Occlusion.* As the duck beak gradually disappears into the back of the elephant, traditional H.D. variants that compare isolated feature matches fail to recognize it. Even the multi-threshold fraction F_{MUT} ranks the house (M-6) above the duck in the barely recognizable E-6, but both Σ_k and +MUL barely make it.

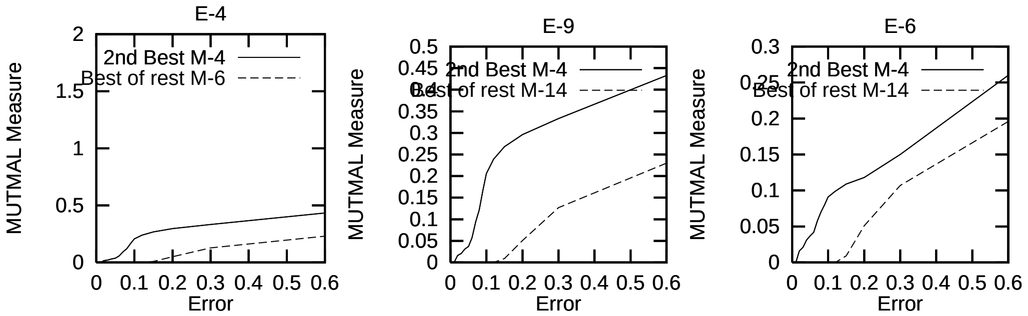

Figure 4: *Effect of increasing occlusion* As occlusion increases, the best match among the non-matching elements approach the second-best match due to increasing noise. The figure also shows the dominance of the Maximal Arc-Length (+MAL) model over other variants.

Fraction model (MUT) and also the Multi-Threshold with Maximal Arc-Length model(+MAL) in the Tables 3,5) and Figures 3.

4.2 Increasing Shape Variation

If the models variation is very high, then it is possible that some other models may contain supersegments that are a better approximation to some of the deformed edges. This is evident in the instance where one of the models (M-9, elephant) has been deformed by 20% Vertex variation. This is a function of the supersegment length ν, however. If ν is increased, the model is easily detected (Table 6). Whereas a different model may accidentally match a sequence of two edges, longer sequences are less likely to be matched. However, greater ν causes greater difficulty at occlusion junctions.

The efficacy of the different Hausdorf model variants as the shape variation increases is shown in Figure 2.

4.3 Increasing Shape Occlusion

The shape E-6 is constructed using only five edge segments of the duck in it; of these two are intersecting. Even human beings can hardly recognize it. This fails with k_th and %k models but can be detected by Σ_k model. In E-9 the duck has some more segments visible hence is detected by k_th model also.

5 Conclusion

We present a novel approach towards shape class modeling and recognition that combines data from multiple levels of confidence and consolidates the results across a broader range of the contour by giving higher weightage to the segments

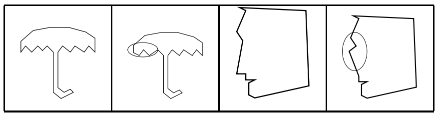

Table 9: Not all variations are equal. While the umbrella is easily recognized, a change of similar magnitude makes the face less recognizable.

that are in corresponding positions in both contours. While the domain of problems chosen - that of 2D polygonal shapes - is somewhat simple, we found in the course of doing this work, that even in this domain, the problem of overlap between highly variant shapes remains a challenging one.

We also present a comparative survey and evaluation of existing Hausdorff Distance models and its variants for comparing feature sets in shape space. It is shown that the MUTMAL model outperforms all existing variants in all recognizable input cases (and also in some practically unrecognizable ones).

A secondary contribution of this paper arises from an observation that not much work is available on the formalization of shape classes as such. Different authors have attempted to model the particular variation encoded by them, and we believe our attempt to formalize the shape variations as variational shape classes may provide a small nucleus towards efforts in formalizing shape variation in terms of deformation.

One of the problems of variational shape recognition is that shape variation may not be uniform over the entire contour, as illustrated in Figure 9. Models for encoding these regions of different "variational tolerance" and then recognizing them remain under-developed in theory and implementation and can be an important area of further research.

References

[1] Ram Bhushan Agrawal, Amitabha Mukerjee, and Kalyanmoy Deb. Modelling of inexact 2-d shapes using real-coded genetic algorithms. In Pradosh K. Roy and Bhishen Singh Mahendra Pal Singh publishers S.D. Mehta, editors, *Proceedings of the Symposium on Genetic Algorithms, March 25 1995, Dehradun, India*, pages 41–49, 1995.

[2] B. Aldefeld. Variation of geometries based on a geometric-reasoning method. *Computer Aided Design, April 1988*, 20(3):117–126, 1988.

[3] Nirwan Ansari and Edward J. Delp. Partial shape recognition: A landmark-based approach. *IEEE Transaction on Pattern Analysis and Machine Intelligence*, 12(5):470–483, May 1990.

[4] Allen R. Tannenbaum Benjamin B. Kimia and Steven W. Zucker. Shapes, shocks, and diffusions i: The components of two-dimensional shape and reaction-diffusion space. Technical report, LEM-Brown, August 1995.

[5] Gregory A. Klanderman Daniel P. Huttenlocher and William J. Rucklidge. Comparing images using the hausdorff distance. *IEEE PAMI*, 15(9):850–862, September 1993.

[6] R. O. Duda and P. E. Hart. *Pattern Classification and Scene Analysis*. Wiley, 1973.

[7] Sven J. Dickinson Kaleem Siddiqi, Ali Shokoufandeh and Steven W. Zucker. Shock graphs and shape matching. Technical Report CVC TR-97-002/CS TR-1147/RU DCS-TR-345, CS, Yale University, October 1997.

[8] Mark W. koch and Rangasami L. Kashyap. Using polygons to recognize and locate partially occluded objects. *IEEE Transcation on Pattern Recognition and Machine Intelligence*, 9(4):483–493, July 1987.

[9] Konstantin Y. Kupeev and Victor L. Brailovosky. A reinforced random algorithm for a partial contour perceptual similarity problem. *Pattern Recognition Letters*, 19:287–297, 1998.

[10] Robert Light and David C Gossard. Modification of geometric models through variational geometry. *CAD, July 1982*, 14(4):209–214, 1982.

[11] Clark F. Olson. A probabilistic formulation for hausdorff matching. In *Proceedings of the IEEE Conference on Computer Vision and Pattern Recognition, Santa Barbara, CA*, pages 150–156, 1998.

[12] Clark F. Olson and Daniel P. Huttenlocher. Automatic target recognition by matching oriented edge pixels. *IEEE Transaction on Image Processing*, 6(1):103–113, January 1997.

[13] A.A.G Requicha and Steve Chan. Representation of geometric features, tolerances, and attributes in solid modelers based on constructive geometry. *IEEE J. Robotics and Automation, September 1986*, RA-2(3):156–166, 1986.

[14] Fridtjof Stein and Gerard Medioni. Structural indexing: Efficient 2-d object recognition. *IEEE Transaction on Pattern Analysis and Machine Intelligence*, 14(12):1198–1204, December 1992.